

Numerical study of the size effect and nucleation center concentration on the elastic properties of copper

Vladyslav Zhykhariev¹, Mariia Shapovalova², Oleksii Vodka³, Serhii Misiura⁴

¹ National Technical University «Kharkiv Polytechnic Institute», Ukraine,
Vladyslav.Zhykhariev@infiz.khpi.edu.ua

² National Technical University «Kharkiv Polytechnic Institute», Ukraine,
Mariia.Shapovalova@khpi.edu.ua

³ National Technical University «Kharkiv Polytechnic Institute», Ukraine,
oleksii.vodka@khpi.edu.ua

⁴ National Technical University «Kharkiv Polytechnic Institute», Ukraine,
serhii.misiura@khpi.edu.ua

Abstract: This article presents the results of a numerical study on the influence of representative volume size and the concentration of initial nucleation centers on the elastic properties of polycrystalline copper, taking into account the anisotropy of its microstructure. The modeling was carried out in a voxel-based system using the finite element method within a numerical analysis environment, applying periodic boundary conditions. This approach enables the simulation of an infinite material structure and avoids edge effects. Three-dimensional geometric models of cubic specimens ranging in size from 5 to 20 voxels were constructed at various concentrations of crystallization points (from 5% to 25%). For each configuration, 100 independent statistical realizations with randomly distributed initial points were performed. This made it possible to obtain reliable estimates of the mean values and variances of the key mechanical properties. The effective values of Young's modulus, shear modulus, and Poisson's ratios were calculated depending on geometric parameters and microstructural variability. The distributions of the obtained values were analyzed using histograms and statistical parameters of the normal distribution. The results showed that increasing the size of the representative volume and the number of crystallization points reduces result variability and leads to convergence towards a stationary mean value. The maximum deviation of Young's modulus across all realizations did not exceed 1.91%, indicating high stability and reproducibility of the calculated properties. It is shown that accounting for anisotropy through an appropriate grain orientation model enables significantly more accurate simulation of polycrystalline material behavior under various loading conditions. The proposed approach can be useful for improving the accuracy of numerical predictions of elastic properties in copper-based components and optimizing technological processes that shape the microstructure. Furthermore, the results can be applied in the design of structural elements with predictable stiffness characteristics, taking into account the internal structure and its influence on the macroscopic behavior of the material.

Keywords: copper, polycrystal, numerical modeling, Young's modulus, size effect, nucleation point concentration, finite element method, statistical evaluation, anisotropy.

1. INTRODUCTION

In the modern world, there is a growing demand for the creation of miniature yet multifunctional systems, which drives scientists toward a deeper study of constitutive behavior at the micro- and nanolevels. At these dimensions, scale-dependent phenomena

become predominant in defining the mechanical properties of materials, such as strength, elasticity, and plasticity. Understanding these phenomena is paramount for the advancement of new technologies and the synthesis of materials with controlled properties, which is a vital task for both science and industry.

Copper, due to its unique properties – specifically its high electrical conductivity and plasticity – holds a prominent place among materials used in various industries. However, its mechanical properties depend significantly on its microstructure, particularly the presence of extraneous inclusions precipitated during production. This aspect often remains insufficiently explored in traditional approaches, highlighting the vital need for new analytical methods to better understand material behavior.

Consequently, the implementation of mathematical models and numerical algorithms plays a crucial role, as they allow for the prediction of changes in elastic properties taking into account the material internal structure, initial crystallization conditions, and anisotropy. The application of such models enables the effective analysis of large volumes of data, the simulation of material behavior under various loads, and the optimization of production processes. Creating algorithms capable of reflecting complex microstructural phenomena allows not only for a deeper understanding of fundamental mechanisms but also for the improvement of the reliability and durability of copper components in high-tech systems.²

2. ANALYSIS OF AVAILABLE RESEARCH

The investigation of the elastic properties of polycrystalline copper, accounting for scale-dependent effects and microstructural peculiarities, remains a cornerstone of modern materials science. Particular emphasis is placed on the influence of grain size on mechanical properties. Specifically, several studies [1–3] have demonstrated that reducing grain size to the 5–15nm range leads to a pronounced decrease in Young's modulus from 130 to 110 GPa due to the increasing proportion of grain boundaries, while at a grain size of 10nm, the shear modulus decreases by 15% due to enhanced creep. In specimens with a broader grain size distribution (5–50nm), Young's modulus reaches only 112GPa, while the Poisson's ratio increases to 0.38, indicating the significant impact of grain boundary on elastic properties. However, despite the importance of these findings, most studies are confined to isotropic representation of the material, neglecting its intrinsic anisotropy.

Research of the impact of inclusions on the elastic properties of copper also reveals notable property shifts. According to [4–8], increasing the concentration of inclusions within a 2–20% range results in a 8–10% reduction in Young's modulus, whereas nanoscale inclusions 5–20nm can enhance ultimate strength by up to 15%, albeit at the cost of reduced plasticity. Furthermore, it has been established that strain hardening in Cu–Ag alloys can increase Young's modulus by 5% due to the deterioration of plastic properties. It should be noted, however, that the majority of research focuses on nanostructured specimens or narrow size ranges, which limits their practical applicability for large-scale materials.

The thermal stability of polycrystalline copper is another critical aspect that determines its service life. According to [9–11], at temperatures exceeding 200 °C, structural stability gradually declines due to grain boundary relaxation, accompanied by a 5-7% reduction in Young's modulus. The introduction of alloying elements, such as phosphorus, enhances thermal stability, though it results in a slight decrease in elastic properties. Concurrently, other studies [12] focusing on the numerical modeling of anisotropic materials and shape memory alloys emphasize the necessity of accounting for complex internal deformation mechanisms when evaluating elastic properties.

Among numerical simulation techniques, the Monte Carlo method is of particular interest. Liu et al. [13] utilized this method to investigate the mechanical properties of porous materials. It was found that while Monte Carlo simulations effectively account for the statistical variability of stochastic processes, they face limitations in the precise description of the microstructure, particularly regarding grain boundaries and their interactions.

An alternative is the voxel modeling approach, based on a three-dimensional representation of the material as an array of voxels. As demonstrated in recent studies [14, 15], the application of a voxel-based model to describe complex structures provides high fidelity in replicating internal geometry, allowing for anisotropy, porosity, defects, and inclusions at the microstructural level to be taken into account. Specifically, this approach enables a detailed numerical evaluation of elastic anisotropy in polycrystalline materials by resolving grain-level interactions [15]. This provides new opportunities for modeling the elastic properties of polycrystalline copper while considering the spatial distribution and orientation of grains.

Unlike the Monte Carlo method and other homogenized or statistical approaches, the voxel model offers a more flexible and detailed description of the material. Its advantages include high-precision geometric reconstruction, compatibility with machine learning frameworks, and the ability to resolve both macro- and micro-scale structural features. This makes the voxel approach highly promising for studying the influence of size effects, inclusion concentration, and thermal stability on the elastic properties of polycrystalline copper.

Thus, the proposed approach, based on voxel modeling and accounting for material anisotropy, variability in initial conditions, and scale-dependent effects – facilitates the acquisition of high-fidelity data regarding the elastic properties of polycrystalline copper. Compared to previous studies, this comprehensive analysis of diverse factors, supported by statistically significant calculations, provides a deeper understanding of the microstructural influence on mechanical behavior, offering significant potential for the refinement of advanced manufacturing technologies.

3. OBJECTIVE OF THE INVESTIGATION

The objective of this study is to evaluate the elastic properties of polycrystalline copper by implementing advanced computational frameworks, taking into account the limitations identified in previous research and leveraging the capabilities of the developed mathematical model. Specifically, the study aims to:

Determine the influence of geometric dimensions of a specimen and the initial nucleation centers concentration on elastic properties.

Ensure statistical validity of the findings by conducting sufficient number of calculations with variable boundary conditions while explicitly accounting for material anisotropy.

Perform numerical stress-strain analysis using specialized software packages to provide a quantitative characterization of the influence of the studied parameters on the mechanical properties of the copper specimen.

Achieving these objectives will facilitate a more profound understanding of the behavior of polycrystalline copper and support the advancement of production technologies for the synthesis of materials with tailored mechanical properties.

4. MATHEMATICAL MODEL

The study uses representative cubic volumes with equilateral geometry. The modeled material is copper. The edge dimensions (S) are defined as 5, 10, 15, and 20 voxels, respectively. Examples of the corresponding are illustrated in Figure 1.

Numerical simulations were performed within a CAE suite, where a static structural analysis was executed for each specific load case. To construct the finite element mesh, a structured mesh utilizing 20-node three-dimensional elements was employed. The total number of nodes after mesh generation depended on the geometric dimensions of the cubic volume.

For the experiment, copper with anisotropic elastic properties was selected, defined by an elasticity tensor, as specified in Table 1 [16].

Table 1. Material properties of copper.

Property	Value (Pa)
$C_{11} = C_{22} = C_{33}$	1.684×10^{11}
$C_{12} = C_{13} = C_{23}$	1.214×10^{11}
$C_{44} = C_{55} = C_{66}$	7.54×10^{10}

For each size of the experimental specimen, the distribution of nucleation centers was simulated at concentrations of 5%, 10%, 15%, 20%, and 25% relative to the total number of nodes in the model.

Representative models of varying sizes and concentrations are shown in (Figure 1). In these figures, color-coded segmentation visualizes the spatial distribution of the nucleation centers corresponding to their concentration relative to the total model volume.

To account for the anisotropic properties of copper, a specific set of local coordinate systems was generated, each characterized by unique Euler angles to define element orientation. This facilitates the modeling of complex anisotropic behavior in different parts of the cube.

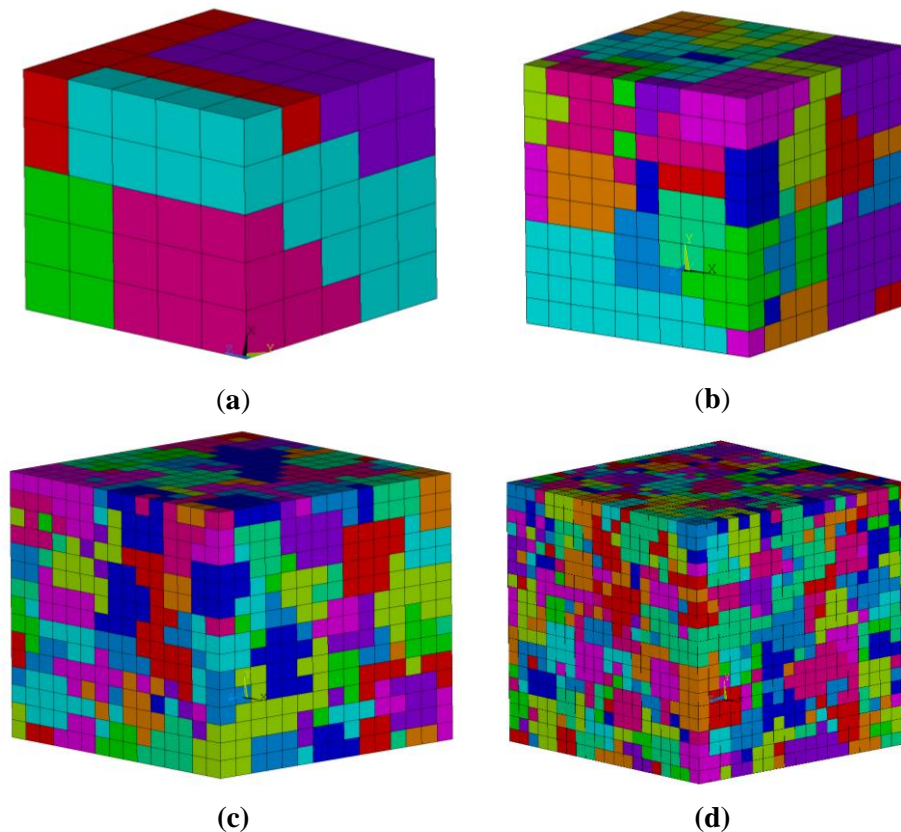


Figure 1. Experimental samples with the following parameters: a) $S=5$ voxels., $\Psi=5\%$; b) $S=10$ voxels, $\Psi=25\%$; c) $S=15$ voxels, $\Psi=15\%$; d) $S=20$ voxels, $\Psi=25\%$.

For each cube size and each concentration, 100 simulations were performed with variable boundary conditions. Displacements (u, v, w) in the X, Y, Z directions were defined by Eq.(1)–(3)

$$u(x, y, z) = \varepsilon_{xx}x + \varepsilon_{xy}y + \varepsilon_{xz}z \quad (1)$$

$$v(x, y, z) = \varepsilon_{yy}y + \varepsilon_{xy}x + \varepsilon_{yz}z \quad (2)$$

$$w(x, y, z) = \varepsilon_{zz}z + \varepsilon_{yz}y + \varepsilon_{xz}x \quad (3)$$

Where x, y, z are the coordinates of the nodes on the faces of a cubic model; $\varepsilon_{xx}, \varepsilon_{yy}, \varepsilon_{zz}$ are the normal deformations in the X, Y, Z directions; $\varepsilon_{xy}, \varepsilon_{xz}, \varepsilon_{yz}$ are shear deformations. The strain values used in Eq. (1)–(3) were generated in the range of -0.001 to 0.001 , simulating various loading scenarios.

In the post-processing part of the numerical experiment, the distributions of displacements, stresses, and strains at the model nodes were obtained. To evaluate the elastic properties of the material, specifically the elastic modulus along the loading direction, Hooke's law for an anisotropic medium was applied as shown in Eq. (4):

$$\sigma_{ij} = C_{ijkl} \varepsilon_{kl} \quad (4)$$

Where: σ_{ij} are the components of the stress tensor; C_{ijkl} are the components of the elasticity tensor; ε_{kl} are the components of the strain tensor.

During the post-processing stage, the distribution of displacements, stresses, and strains at the nodes of the numerical model was obtained.

The results of each calculation were saved in a CSV file for further processing.

The file format includes coordinates of the displacements, stresses, and strains for each node under the imposed boundary conditions.

The obtained results allow for an evaluation of the influence of the experimental specimen size and the nucleation centers concentration on the mechanical properties of the material, particularly on the stress and strain distribution. A specimen of 100 calculations for each combination of size and concentration allows for accounting for statistical variability and determining patterns in the behavior of the material.

5. RESULTS

The results of the Von Mises stress distribution for several experimental specimens are presented in (Fig. 2). (Fig. 2b) shows the stress distribution for a representative volume of 10 voxels with a concentration of 25%, where maximum stresses are observed in areas with a high density of nucleation centers. Similarly, (Fig. 2d) depicts the distribution for a 20-voxel specimen with a 25% concentration, where the stresses are distributed more uniformly, indicating more stable behavior of the material.

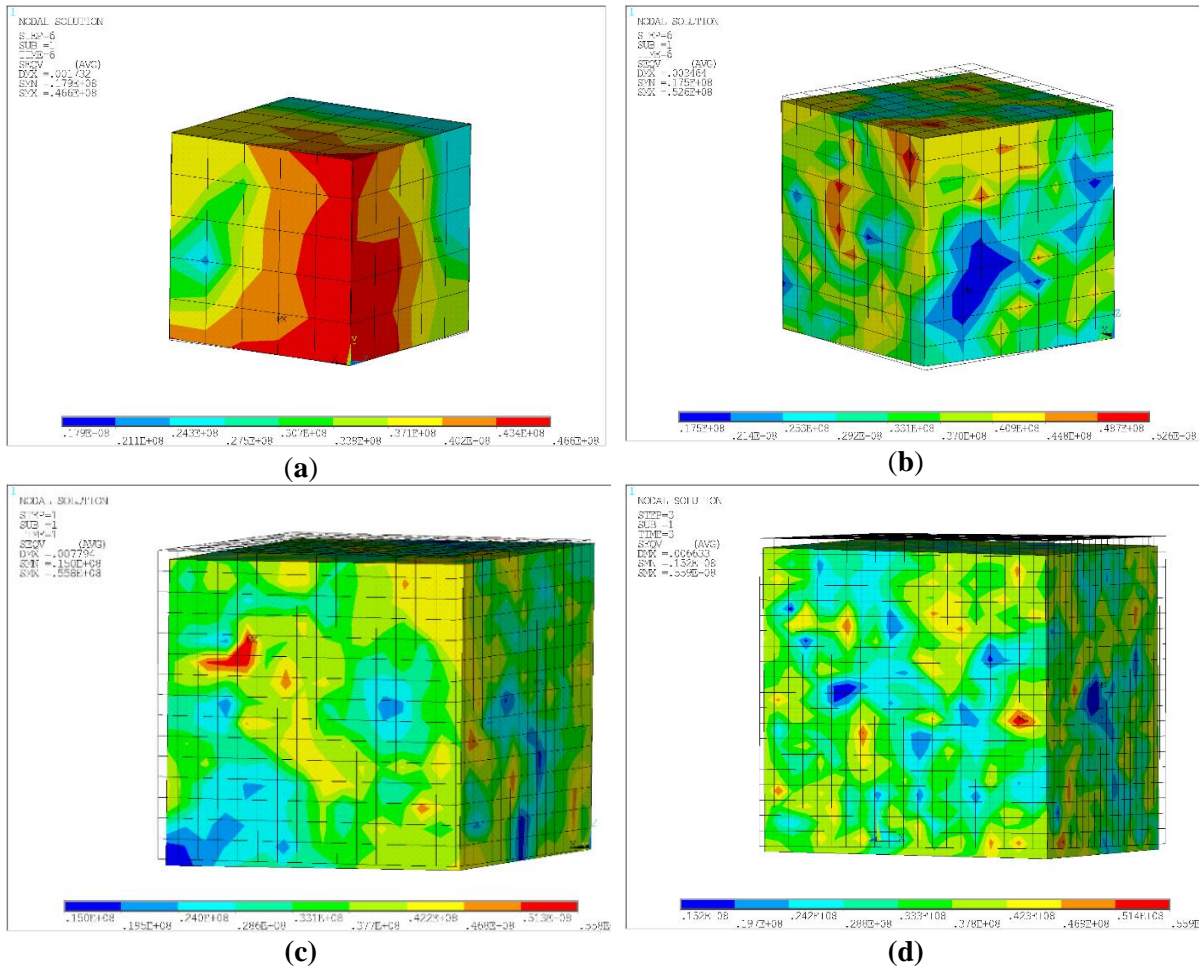


Figure 2. Von Mises stress distribution for the model: a) S=5 voxels, Ψ =5%; b) S=10 voxels, Ψ =25%; c) S=15 voxels, Ψ =15%; d) S=20 voxels, Ψ =25%.

To evaluate the influence of the nucleation center concentration on the elastic properties of the copper plate, the elastic modulus (E), Poisson’s ratio (ν), and shear modulus (G) were analyzed. For each concentration (5%, 10%, 15%, 20%, 25%), the mean values of these properties were calculated based on 100 simulations for each specimen size. The results are presented as dependency graphs in (Fig. 3), where the deviation from the mean values is shown as confidence intervals, calculated using the formula:

$$\alpha_{int} = \underline{x} \pm 3\sqrt{D} \tag{5}$$

Where \underline{x} is the mean value of the property, D is the variance, and the factor 3 corresponds to 99.7% probability for a normal distribution.

$$D = \frac{1}{N} \sum_{i=1}^N (x_i - \underline{x})^2 \tag{6}$$

Where N is the number of calculations (in our case, N=100); x_i is the value of the property for the i-th calculation; \underline{x} is the mean value of the property, calculated as $\underline{x} = \frac{1}{N} \sum_{i=1}^N x_i$

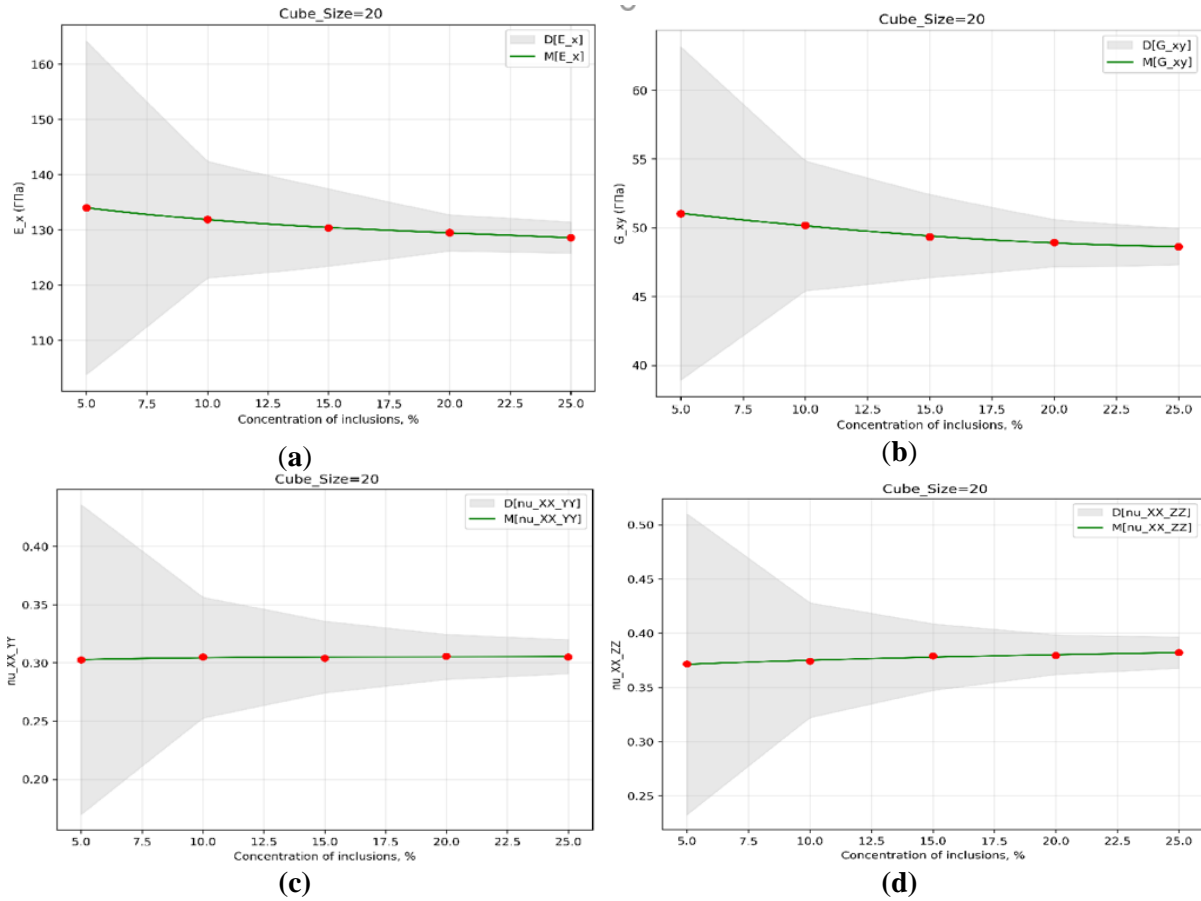


Figure 3. Dependence of elastic properties: a) Young’s modulus E_x ; b) shear modulus G_{xy} ; c) Poisson’s ratios ν_{xy} ; d) ν_{xz} in the concentration of inclusions at a fixed size of 20 voxels.

The averaged values of elastic properties for all sizes and concentrations, along with the corresponding variances, are given in (Table 2). The averaging is based on the results of 100 calculations for each combination of size and concentration.

Table 2. Mean values of elastic properties and their dispersion.

S	Ψ	M		D		M		D		M		D	
		$[E_x]$	$[E_x]$	$[E_y]$	$[E_y]$	$[E_z]$	$[E_z]$	$[G_{xy}]$	$[G_{xy}]$	$[\nu_{xy}]$	$[\nu_{xy}]$	$[\nu_{xz}]$	$[\nu_{xz}]$
		GPa						10^{-3}					
5	5	131.3	3.80	132.1	5.67	123.5	61.2	50.00	4.84	0.301	4.28	0.37	4.32
5	10	132.2	3.09	132.9	2.67	123.2	6.24	50.00	5.84	0.299	0.68	0.38	0.70
5	15	131.4	1.03	132.0	1.22	122.0	3.52	49.93	4.06	0.302	0.27	0.38	0.23
5	20	129.6	3.79	129.9	4.78	120.6	2.27	49.92	1.06	0.305	0.13	0.38	0.10
5	25	128.9	1.29	129.9	5.20	119.9	1.72	49.87	5.20	0.305	0.06	0.38	0.06
10	5	135.3	1.48	135.2	1.53	126.3	14.6	49.60	2.57	0.298	3.92	0.37	4.23
10	10	132.6	3.91	132.4	1.81	123.1	5.84	49.92	3.91	0.300	0.46	0.38	0.53
10	15	130.6	1.21	130.6	4.95	121.	3.40	49.87	1.79	0.303	0.15	0.38	0.18
10	20	129.5	2.32	129.6	1.35	120.0	1.96	49.87	3.88	0.305	0.07	0.38	0.06

10	25	128.7	1.24	128.6	1.35	119.5	1.43	49.82	2.12	0.305	0.03	0.38	0.03
15	5	131.9	1.71	130.6	1.20	122.4	12.6	50.00	2.96	0.297	3.25	0.38	2.87
15	10	131.3	1.63	130.6	1.98	122.7	4.56	49.99	3.47	0.300	0.40	0.38	0.37
15	15	129.4	4.87	129.4	8.82	121.2	2.67	49.88	2.30	0.306	0.12	0.38	0.11
15	20	129.6	8.84	129.4	1.53	120.4	1.69	49.87	2.58	0.305	0.05	0.38	0.04
15	25	128.6	1.24	128.6	1.35	119.6	1.10	49.84	2.12	0.305	0.03	0.38	0.02
20	5	134.0	1.01	131.6	1.63	125.4	11.5	50.09	2.48	0.302	1.97	0.37	2.14
20	10	131.3	5.24	130.2	5.71	123.2	4.29	49.53	1.01	0.303	0.30	0.38	0.31
20	15	130.4	1.95	129.3	1.52	121.1	2.47	49.83	2.37	0.305	0.11	0.38	0.10
20	20	129.3	1.95	129.3	1.52	120.4	1.46	49.44	2.37	0.305	0.04	0.38	0.04
20	25	129.3	1.95	129.3	1.52	119.4	1.20	49.43	2.37	0.305	0.02	0.38	0.02

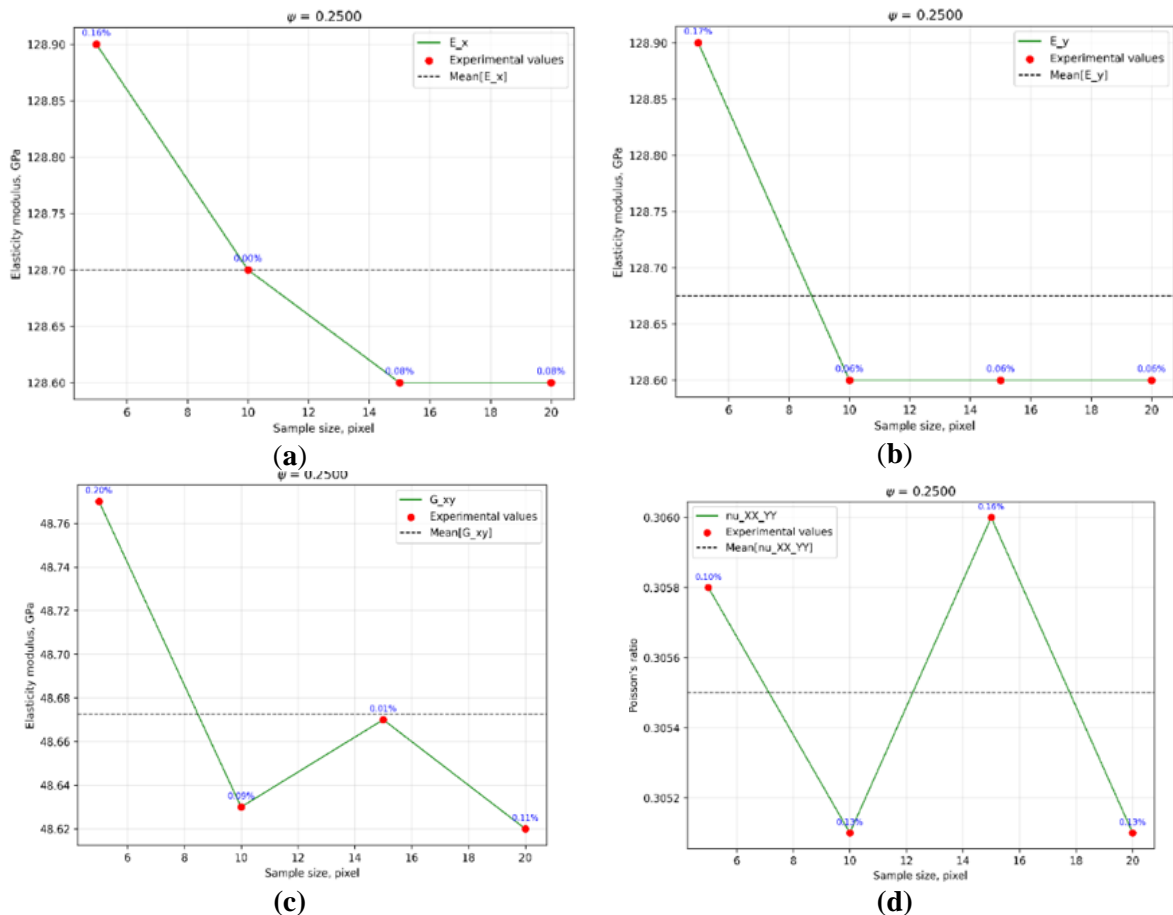


Figure 3. Dependence of elastic properties: a) Young's modulus E_x ; b) E_y ; c) shear modulus G_{xy} ; d) Poisson's ratio ν_{xy} on the sizes of the studied volumes at a concentration of 25% of the nucleation centers.

To evaluate the scale effect, the dependence of elastic properties on the size of the test specimen was analyzed. The graphs showing the dependence of the elastic modulus (E), Poisson's ratio (ν), and shear modulus (G) on the size of the representative volume for a concentration of 25% are presented in (Fig. 6). These graphs also indicate the maximum deviations from the mean values of the elastic properties.

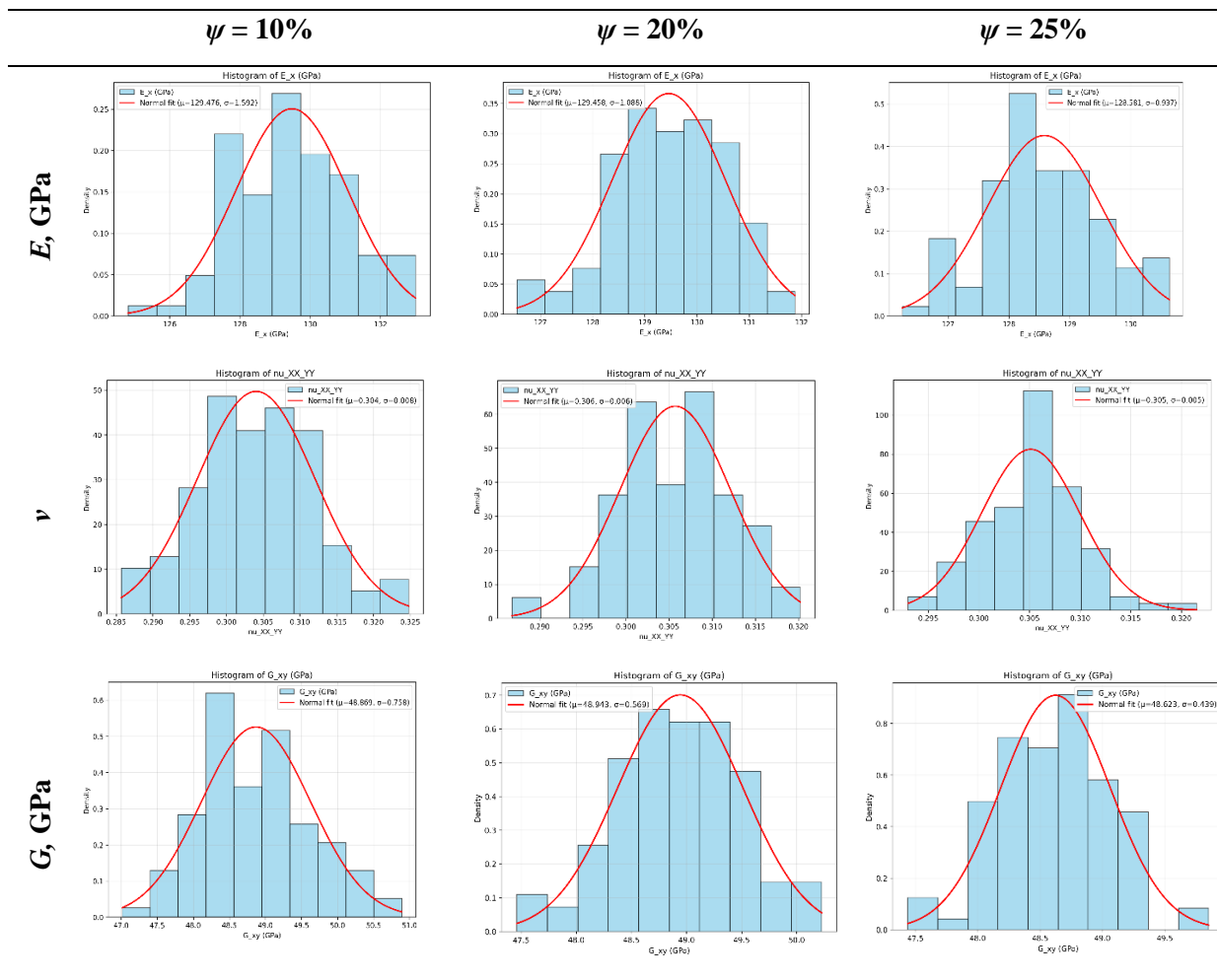
Table 3 presents the deviations for all experiments. According to the data, the deviations of the elastic properties from the mean values are insignificant (maximum 1.91%, mean 0.1%–0.6%), which indicates high material stability under varying experimental specimen sizes and concentrations. The largest deviations are observed at a concentration of $\Psi=5\%$ (up to 1.91%), while the smallest occur at higher concentrations (15%–25%).

Table 3. Maximum deviations of elastic properties for different S and Ψ .

<i>S</i>	Ψ	E_x	E_y	E_z	G_{xy}	G_{xz}	G_{yz}	ν_{xxyy}	ν_{xxzz}	ν_{yyzz}
(voc)	%	Maximum deviations, %								
5	5	1.43	0.84	0.72	1.09	1.47	1.70	0.97	0.47	1.05
5	10	0.04	0.53	0.12	0.06	0.55	0.10	0.70	0.50	0.28
5	15	0.54	0.48	0.45	0.07	0.05	0.10	0.30	0.20	0.11
5	20	0.25	0.10	0.21	0.60	0.38	0.04	0.30	0.07	0.55
5	25	0.16	0.17	0.25	0.20	0.04	0.08	0.10	0.21	0.19
10	5	1.65	1.48	1.53	1.50	0.70	0.79	0.89	0.71	0.20
10	10	0.34	0.15	0.04	0.22	0.09	0.15	0.40	0.05	0.31
10	15	0.08	0.06	0.04	0.01	0.03	0.06	0.13	0.02	0.11
10	20	0.06	0.06	0.29	0.26	0.05	0.26	0.39	0.27	0.47
10	25	0	0.06	0.08	0.09	0.01	0.01	0.13	0.10	0.12
15	5	0.83	0.92	1.61	1.26	1.73	1.91	0.86	1.40	1.69
15	10	0.19	0.23	0.28	0.04	0.02	0.15	0.03	0.13	0.25
15	15	0.23	0.06	0.21	0.11	0.03	0.10	0.10	0.24	0.03
15	20	0.14	0.02	0.04	0.23	0.17	0.09	0.09	0.02	0.11
15	25	0.08	0.06	0	0.01	0.11	0.11	0.16	0.08	0.09
20	5	0.60	0.28	0.80	1.34	0.44	0.57	0.77	1.16	0.44
20	10	0.19	0.45	0.12	0.32	0.44	0.19	1.06	0.67	0.28
20	15	0.23	0.36	0.29	0.03	0.11	0.05	0.26	0.02	0.18
20	20	0.06	0.06	0.04	0.11	0.25	0.13	0.17	0.18	0.03
20	25	0.08	0.06	0.02	0.11	0.06	0.02	0.13	0.18	0.15

To evaluate the distribution of elastic properties, histograms were constructed for the elastic moduli ($E_x, E_y, E_z, G_{xy}, G_{xz}, G_{yz}$) and Poisson’s ratios ($\nu_{xxyy}, \nu_{xxzz}, \nu_{yyzz}, \nu_{xxyy}, \nu_{yyyy}, \nu_{zzxz}$) at a model size of 20 voxels (Table 4). Normal distribution curves with corresponding mean values (μ) and standard deviations (σ) were superimposed on the histograms to evaluate the compliance of the data to a normal distribution. The 20-voxel model was selected due to having the lowest mean variance (1.38) compared to other experimental specimens, which ensures maximum stability of the properties and makes it optimal for distribution analysis.

Table 4. Histogram of the distribution of elastic modulus, Poisson’s ratio, and shear modulus.



6. CONCLUSIONS

As a result of numerical modeling, it was established that the nucleation center concentration and specimen size exert a limited influence on the elastic properties of polycrystalline copper. This is evidenced by negligible deviations from the mean values, with a maximum of 1.91% and an average range of 0.1%–0.6%. The highest stability of properties is observed at a representative volume size with a side length of $S=20$ voxels (mean variance of 1.38) and inclusion concentrations of 15%–25%, where the von Mises criterion is more uniform compared to smaller sizes (e.g., 10 voxels). The obtained results indicate that the scale effect associated with changes in specimen size tends to reduce the variation in elastic properties as the size increases. Histograms of the distribution of elastic moduli for the 20-voxel size confirm that the data follows a normal distribution, highlighting the statistical reliability of the results. The largest deviations (up to 1.91%) are observed at a concentration of 5%, which may be attributed to lower homogeneity of the material structure at low nucleation center concentrations. These findings deepen the understanding of scale effects in polycrystalline materials and can be utilized to optimize manufacturing technologies for copper components with specified mechanical properties, particularly in micro- and nanotechnology.

REFERENCES

- [1] R. Kumar, M.K. Gupta, S.K. Rai, V. Panwar, Grain size responsive uniaxial tensile behavior of polycrystalline nanocopper under different temperatures and strain rates, *Multidiscipline Modeling in Materials and Structures*. 19 (2023) 507–521. <https://doi.org/10.1108/MMMS-09-2022-0187>.
- [2] G.W. Nieman, J.R. Weertman, R.W. Siegel, Mechanical Behavior of Nanocrystalline Cu and Pd, *J. Mater. Res.* 6 (1991) 1012–1027. <https://doi.org/10.1557/JMR.1991.1012>.
- [3] M.Y. Shen, J.R. Lloyd, Modeling the Copper Microstructure and Elastic Anisotropy and Studying Its Impact on Reliability in Nanoscale Interconnects, *Mech. Adv. Mater. Mod. Process.* 3 (2017) 6. <https://doi.org/10.1186/s40759-017-0021-z>.
- [4] Y. Geng, Y. Ban, B. Wang, X. Li, K. Song, Y. Zhang, Y. Jia, B. Tian, Y. Liu, A. Volinsky, Review of Microstructure and Texture Evolution with Nanoscale Precipitates for Copper Alloys, *J. Mater. Res. Technol.* 9 (2020) 11918–11934. <https://doi.org/10.1016/j.jmrt.2020.08.055>.
- [5] T. Böhlke, A. Bertram, Asymptotic Values of Elastic Anisotropy in Polycrystalline Copper for Uniaxial Tension and Compression, *Int. J. Solids Struct.* 91 (2016) 123–134.
- [6] Z. Li, K. Chen, X. Zhu, Y. Chen, M. Wang, Y. Shen, J. Shi, J. Wang, Z. Wang, In-Situ Fabrication, Microstructure and Mechanical Performance of Nano Iron-Rich Precipitate Reinforced Cu and Cu Alloys, *Metals*. 12 (2022) 1453. <https://doi.org/10.3390/met12091453>.
- [7] M. Xie, W. Huang, H. Chen, L. Gong, W. Xie, H. Wang, B. Yang, Microstructural Evolution and Strengthening Mechanisms in Cold-Rolled Cu–Ag Alloys, *J. Alloys Compd.* 851 (2021) 156893. <https://doi.org/10.1016/j.jallcom.2020.156893>.
- [8] L. Ladani, J. Razmi, T.C. Lowe, Manufacturing of High Conductivity, High Strength Pure Copper with Ultrafine Grain Structure, *J. Manuf. Mater. Process.* 7 (2023) 137. <https://doi.org/10.3390/jmmp7040137>.
- [9] C. Saldana, A.H. King, S. Chandrasekar, Thermal Stability and Strength of Deformation Microstructures in Pure Copper, *Acta Mater.* 60 (2012) 4107–4116. <https://doi.org/10.1016/j.actamat.2012.04.022>.
- [10] C.F. Gu, C.H.J. Davies, Thermal Stability of Ultrafine-Grained Copper During High Speed Micro-Extrusion, *Mater. Sci. Eng. A*. 527 (2010) 1791–1799. <https://doi.org/10.1016/j.msea.2009.11.005>.
- [11] V.M. Senkivskyi, Z.I. Pikh, N.V. Yavorska, M. Lewandowska, Modeling of Fatigue Crack Growth in Shape Memory Alloys, *Sci. J. Ternopil Natl. Tech. Univ.* 98 (2020) 5–14 https://doi.org/10.33108/visnyk_tntu2020.03.005.
- [12] S.D. Tekade, K.N. Patil, Physical properties of Cu nanoparticles: A molecular dynamics study, in: *Proceedings of the International Conference on Nanotechnology (ICN)*, 2013, pp. 1–5. <https://doi.org/10.1016/j.matchemphys.2014.04.030>.
- [13] Z. Liu, S. Wu, Y. Li, Mechanical Behavior Analysis of Porous Materials Using Monte Carlo Simulation, *Appl. Sci.* 12 (2022) 575. <https://doi.org/10.3390/app12020575>.
- [14] L. Wang, X. Liu, J. Zhang, Microstructure-based numerical modeling of elastic anisotropy in polycrystalline copper, *Mater. Charact.* 202 (2023) 113028. <https://doi.org/10.1016/j.matchar.2023.113142>.
- [15] A. Vázquez, A. Alonso, C. Castro, J. León, Voxel-Based Modeling for the Mechanical Characterization of 3D-Printed Structures, *Materials*. 14 (2021) 5670. <https://doi.org/10.3390/ma14195670>.
- [16] H.M. Ledbetter, E.R. Naimon, Elastic Properties of Metals and Alloys, II. Copper, *J. Phys. Chem. Ref. Data*. 3 (1974) 897–935.